

# R-parity violating resonant stop production at the Large Hadron Collider

---

**Nishita Desai<sup>a</sup> and Biswarup Mukhopadhyaya<sup>a,b</sup>**

*<sup>a</sup>Regional Centre for Accelerator-based Particle Physics,  
Harish-Chandra Research Institute  
Chhatnag Road, Jhansi,  
Allahabad - 211 019, India*

*<sup>b</sup>Indian Association for Cultivation of Science,  
Raja SC Mullick Road,  
Jadavpur, Kolkata - 700032, India  
Email: nishita@hri.res.in, biswarup@hri.res.in*

**ABSTRACT:** We have investigated the resonant production of a stop at the Large Hadron Collider, driven by baryon number violating interactions in supersymmetry. We work in the framework of minimal supergravity models with the lightest neutralino being the lightest supersymmetric particle which decays within the detector. We look at various dilepton and trilepton final states, with or without b-tags. A detailed background simulation is performed, and all possible decay modes of the lighter stop are taken into account. We find that higher stop masses are sometimes easier to probe, through the decay of the stop into the third or fourth neutralino and their subsequent cascades. We also comment on the detectability of such signals during the 7 TeV run, where, as expected, only relatively light stops can be probed. Our conclusion is that the resonant process may be probed, at both 10 and 14 TeV, with the R-parity violating coupling  $\lambda''_{312}$  as low as 0.05, for a stop mass of about 1 TeV. The possibility of distinguishing between resonant stop production and pair-production is also discussed.

**KEYWORDS:** MSSM, supersymmetry, R-parity violation.

---

## Contents

<b>1. Introduction</b>	<b>1</b>
<b>2. Resonant stop production and decays</b>	<b>4</b>
2.1 Stop production	4
2.2 Stop decays and choice of benchmark points	5
<b>3. Event generation and selection</b>	<b>8</b>
3.1 Event generation	8
3.2 Event selection	8
<b>4. Results</b>	<b>10</b>
4.1 Limits at $\sqrt{s}=14, 10$ TeV	10
4.2 Observability at the early run of 7 TeV	14
4.3 Differentiating from R-conserving signals	14
<b>5. Non-<math>\tilde{\chi}_1^0</math> LSPs</b>	<b>15</b>
<b>6. Summary and Conclusion</b>	<b>16</b>

---

## 1. Introduction

The current structure of the standard model (SM), with gauge invariance and renormalisability built in, implies automatic lepton and baryon number conservation. This is no longer true in the supersymmetric (SUSY) extension of the SM [1, 2], where scalars carrying baryon or lepton number are present. Thus the superpotential of the minimal SUSY standard model (MSSM), namely

$$\mathcal{W}_{MSSM} = h_{ij}^d Q_i D_j^c H_d + h_{ij}^u Q_i U_j^c H_u + h_{ij}^l L_i E_j^c H_d + \mu H_u H_d \quad (1.1)$$

can in principle be augmented to include

$$\mathcal{W}_{RPV} = \mu_i L_i H_u + \lambda_{ijk} L_i L_j E_k^c + \lambda'_{ijk} L_i Q_j D_k^c + \lambda''_{ijk} U_i^c D_j^c D_k^c \quad (1.2)$$

which contain terms that are gauge invariant and renormalisable but explicitly violate lepton or baryon number. Here,  $L(E)$  is an  $SU(2)$  doublet (singlet) lepton superfield and  $Q(U,D)$  is (are) an  $SU(2)$  doublet (singlet) quark superfield(s).  $H_u$  and  $H_d$  are the two Higgs doublet superfields,  $\mu$  is the Higgsino parameter and  $(i, j, k)$  are flavour indices. Each

term in equation (1.2) violates R-parity, defined as  $R = (-1)^{3(B-L)-2S}$  (where B is baryon number, L is lepton number and S is spin), against which all SM particles are even whereas all superpartners are odd. The consequence of violating R-parity is that superpartners need not be produced in pairs anymore, and that the lightest superparticle (LSP) can now decay. The strongest argument for studying R-parity violation is that it does not arise as an essential symmetry of MSSM. However, the requirement of suppressing proton decay prompts one to allow *only one* of B and L to be violated at a time.

The collider phenomenology in the absence of R-parity may be very different from that of the usual R-parity conserving MSSM. In particular, if the R-parity violating (RPV) couplings are large enough, the LSP will decay within the detector and one no longer has missing- $E_T$  as a convenient discriminator. Although studies have taken place on such signals, closer looks at them are often quite relevant in the wake of the Large Hadron Collider (LHC). In particular, it is crucial to know the consequences of broken R-parity in the production of sparticles. Here we perform a detailed simulation in the context of the LHC, highlighting one possible consequence of the B-violating term(s), namely, the resonant production of a squark—in this case, the stop.

Many of the RPV couplings have been indirectly constrained from various decay processes, including rare and flavour-violating decays and violation of weak universality. The constraints derived are of two general kinds—those on individual RPV couplings, assuming the existence of a single RPV term; and those on the products of couplings when at least two terms are present, which contribute to some (usually rare) process. The constraints obtained so far are well-listed in the literature[3].

The L-violating terms are relatively well-studied, partly because of their potential role in generating neutrino masses and are constrained by indirect limits. In comparison, the baryon-number violating coupling are relatively unconstrained.  $\lambda''_{112,113}$  are constrained from double nucleon decay and neutron-antineutron oscillations[4, 5, 6]. The rest of the couplings are constrained only by the requirement that they remain perturbative till the GUT scale. Limits on  $\lambda''_{3ij}$  type of couplings due to the ratio of Z-boson decay widths for hadronic versus leptonic final states have been calculated for a stop mass of 100 GeV [7]. However, the results do not restrict the couplings for high stop masses of concern here. The coupling  $\lambda''_{3jk}$  is thus practically unconstrained for large stop masses. It is also known that mixing in the quark sector causes generation of couplings of different flavour structures and can therefore be constrained by data from flavour changing neutral currents(FCNC)[8]. Such effects arising from mixing in the quark and squark sector can affect the contribution of R-parity violation to physical process and alter the limits[9]. However these effects are model dependent and have not been taken into account here.

It has been already noticed that such large values of  $\lambda''$ -type couplings as are still allowed, not only cause the LSP to decay, but also lead to resonant production of squarks via quark fusion at the LHC. The rate of such fusion can in fact far exceed that of the canonically studied squark-pair production. One would therefore like to know how detectable the resonant process is at the LHC. Furthermore, one needs to know the search limits in different phases of the LHC, and how best to handle the backgrounds, both from the SM and the R-conserving SUSY processes. These are some of the questions addressed in this

paper.

Single stop production, mostly in the context of the Tevatron, was studied in detail in [10, 11]. A full one-loop production cross section can be found in [12]. A study of SUSY with the LSP decaying through baryon-number violating couplings and therefore giving no missing energy was done in [13]. Further studies on determining the flavour structure of baryon number violating couplings and possible mass reconstruction following specific decay chains can be found in [14, 15]. There have also been recent studies on possible LSPs [16] and identification of R-parity violating decays of the LSP using jet substructure methods [17]. A recent study on identification of stop-pair production via top-tagging using jet-substructure can be found in [18].

We find, however, that the earlier studies on resonant stop production are inadequate in the context of the LHC. We improve upon them in the following respects:

- In the work done for the Tevatron, the sparticle masses were required to be less than 500 GeV to be within reach. Thus, the gluino was also required to be much lighter than a TeV to avoid large radiative corrections to squark masses. This implied that in the constrained MSSM (cMSSM) [19] scenario, the LSP, assumed to be the lightest neutralino ( $\tilde{\chi}_1^0$ ), had to have mass less than 100 GeV. If we allow only the term proportional to  $\lambda''_{3ij}$ , the only three-body decay of  $\tilde{\chi}_1^0$  is  $\tilde{\chi}_1^0 \rightarrow \bar{t}\bar{d}_i\bar{d}_j(tds)$ . Since the neutralino is much lighter than the top, it can decay only via a 4-body decay and therefore has long lifetime and decays outside the detector for all allowed values of  $\lambda''_{3ij}$  [20]. Thus, one still has the canonical missing- $E_T$  signature. This was one of the main assumptions in [11]. However, if the stop mass is beyond the Tevatron reach but within the reach of the LHC, we may indeed have lightest-neutralino mass high enough to allow decay within the detector.
- We focus on this richer and more challenging scenario within the framework of minimal supergravity (mSUGRA) models. We investigate the LHC reach for detection of the lightest stop assuming that the lightest neutralino is the LSP which decays within the detector and the stop is heavy enough to be beyond the reach of Tevatron.
- For a light stop, the only available R-parity conserving decay modes are into the lightest neutralino ( $\tilde{\chi}_1^0$ ) and lighter chargino ( $\tilde{\chi}_1^\pm$ ) i.e.  $\tilde{t} \rightarrow t\tilde{\chi}_1^0, b\tilde{\chi}_1^\pm$ . For stop mass near a TeV, the decay modes into higher neutralinos and the heavier chargino may open up, leading to different final states. We have found that this drastically improves the detectability of the signature over the SM backgrounds.
- We have taken into account all the potential backgrounds at the LHC, including those from  $t\bar{t} + jets, Wt\bar{t} + jets, Zt\bar{t} + jets$ , which pose little problem at the Tevatron. A detailed investigation towards reducing these backgrounds has been reported in the present study.
- In identifying signals of stop decay, it is often helpful to tag b quarks. This is especially important since the reconstruction of energetic top quarks in multi-top final states is difficult and has a low efficiency. However, the b-jets produced from

stop decay can be quite hard, especially when the stop is heavy and one is looking at the decay in the  $b\tilde{\chi}_1^+$  channel. It is not clear that the b-tagging efficiency is appreciable at the LHC for b-jets with  $p_T \gtrsim 100$  GeV. With this in mind, we have performed a conservative analysis with a b-jet has zero detection efficiency unless its  $p_T$  lies in the range 50 - 100 GeV[21].

We present our results for centre of mass energies of 7, 10 and 14 TeV at the LHC. In section 2, we discuss the rates for resonant stop production, the different decays of the stop and our choice of benchmark points to account for all of them. In section 3, we present a detailed description of cuts required to isolate the signal and section 4 contains the numerical results from our simulation. We also comment on the distinguishability of such a signal from dilepton signals coming from R-parity conserving MSSM. It is possible to have LSPs other than  $\tilde{\chi}_1^0$  when R-parity is violated. We comment on the possibility of detection in such cases in section 5 and summarise and conclude in section 6.

## 2. Resonant stop production and decays

### 2.1 Stop production

The resonant stop production process depends on B-violating couplings proportional to  $\lambda''_{3ij}$ , and also on fraction of the right-chiral eigenstate ( $\tilde{t}_R$ ) in the mass eigenstate concerned. We concentrate on the production of  $\tilde{t}_1$  since the lighter stop eigenstate usually has a higher fraction of  $\tilde{t}_R$ . The resonant production cross section is given by

$$\sigma_{\tilde{t}_1} = \frac{2\pi \sin^2 \theta_{\tilde{t}}}{3m_{\tilde{t}}^2} \times \sum_{i,j} |\lambda''_{3ij}|^2 \int dx_1 dx_2 [f_i(x_1) f_j(x_2) + f_i(x_2) f_j(x_1)] \delta(1 - \frac{m_{\tilde{t}_1}}{\sqrt{s}}) \quad (2.1)$$

where  $\sin \theta_{\tilde{t}}$  is the amplitude of finding a  $\tilde{t}_R$  in  $\tilde{t}_1$ ,  $f_i$  is the proton parton distribution function for a parton of species  $i$  and  $x_{(1,2)}$  are the momentum fractions carried by the respective partons. Out of the three possible  $\lambda''$  couplings, contributions via  $\lambda''_{313}$  and  $\lambda''_{323}$  are suppressed due to the small fraction of b quarks in the proton. We therefore look at the production of top (anti) squark through the fusion of the d and s (anti)quarks, via the coupling  $\lambda''_{312}$ . Since the actual cross section for production of the lightest stop depends on the mixing angle via  $\sin^2 \theta_{\tilde{t}}$ , it is useful to define the cross section in terms of an effective coupling  $\lambda''_{eff} = \sin \theta_{\tilde{t}} \lambda''_{312}$ .

$$\sigma_{\tilde{t}_1} = \frac{2\pi}{3m_{\tilde{t}_1}^2} |\lambda''_{eff}|^2 \times 2 \int dx_1 dx_2 [f_d(x_1) f_s(x_2) + f_d(x_2) f_s(x_1) + f_{\bar{d}}(x_1) f_{\bar{s}}(x_2) + f_{\bar{d}}(x_2) f_{\bar{s}}(x_1)] \delta(1 - \frac{m_{\tilde{t}_1}}{\sqrt{s}}) \quad (2.2)$$

The production cross section at the LHC with centre-of-mass energies of 7, 10 and 14 TeV is given in Figure 1. As an illustration, we have chosen the value  $\lambda''_{eff} = 0.2$  which is consistent with the existing limit on  $\lambda''_{312}$ . In general, both  $\tilde{t}_1$  and  $\tilde{t}_2$  will be produced. However, due to larger mass and smaller fraction of  $\tilde{t}_R$ ,  $\tilde{t}_2$  is rarely produced. For comparison, we also present the  $\tilde{t}_1$ -pair production cross-section via strong interaction. For  $m_{\tilde{t}_1} > 500$  GeV, the resonant production dominates over pair-production for  $\lambda''_{eff} > 0.01$  at 14 TeV. Resonant production can therefore hold the key to heavy stop signals if baryon number is violated.

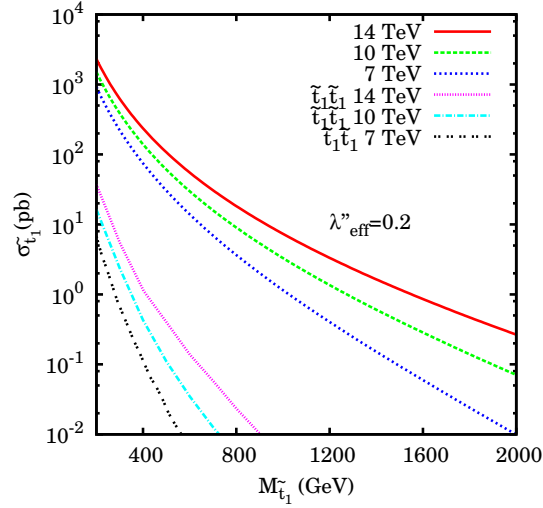


**Figure 1:** Production cross section at the LHC for  $\sqrt{s} = 7, 10$  and 14 TeV with  $\lambda''_{eff} = 0.2$ . The corresponding cross sections for R-conserving pair production are also shown.

At next-to-leading order, the production cross section at  $\sqrt{s} = 14$  TeV is modified by a k-factor of about 1.4[12]. The uncertainty due to renormalisation and factorisation scales at lowest order is about 10% and drops to 5% when NLO corrections are taken into account.

## 2.2 Stop decays and choice of benchmark points

We wish to make our conclusions apply broadly to a general SUSY scenario and to include all possible final states arising from stop decay. However, the multitude of free parameters in the MSSM often encourages one to look for some organising principle. A common practice in this regard is to embed SUSY in high-scale breaking scheme. Following this practice, we have based our calculation on the minimal supergravity (mSUGRA) model[22], mainly for illustrating our claims in a less cumbersome manner. The high scale parameters in this model are:  $m_0$ , the unified scalar parameter,  $m_{1/2}$ , the unified gaugino parameter,  $sign(\mu)$ , where  $\mu$  is the Higgsino mass parameter,  $A_0$ , the unified trilinear coupling and  $\tan\beta$ , the ratio of the two Higgs vacuum expectation values.

Although the production cross section of the stop depends only on the mass and mixing angle of the stop, any strategy developed for seeing the ensuing signals has to take note

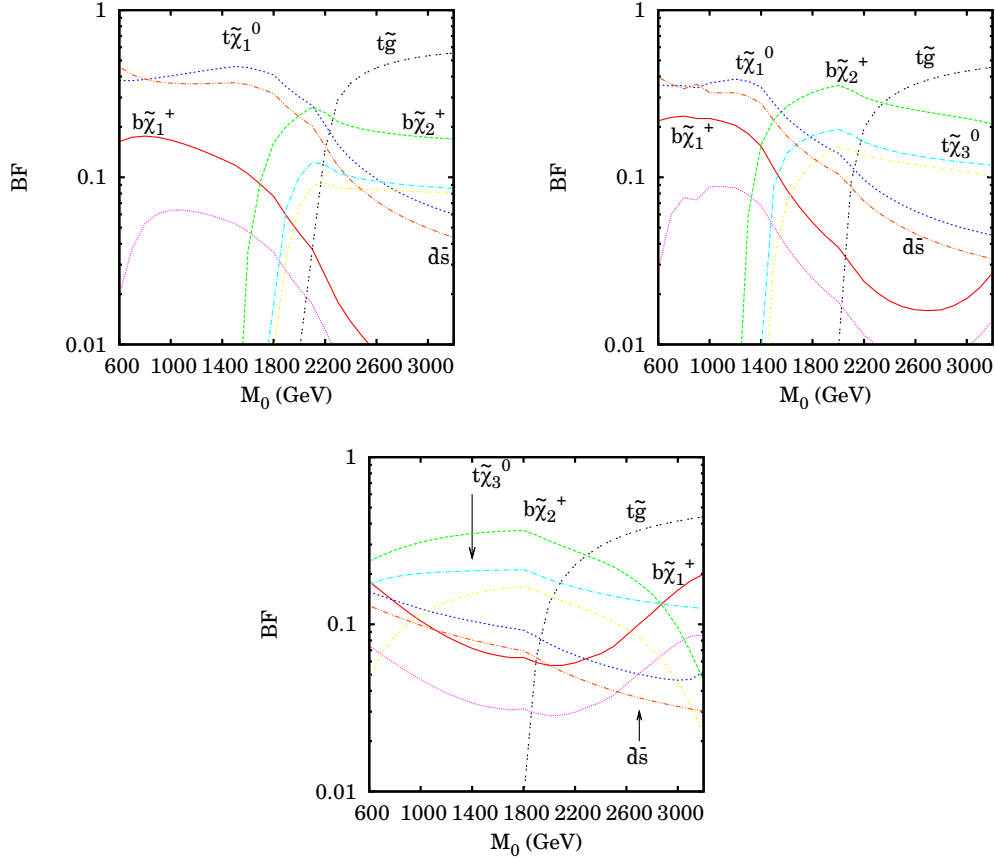


**Figure 2:** Lighter stop decay branching fractions in different modes for  $\tan \beta = 5$ ,  $A_0 = -1500$  (top left) ;  $\tan \beta = 40$ ,  $A_0 = -1500$  (top right) and  $\tan \beta = 10$ ,  $A_0 = 0$  (bottom).  $\lambda''_{312} = 0.2$ ,  $\mu > 0$  and  $m_{1/2} = 450$  GeV in all cases.

of the decay channels. We have tried to make our analysis comprehensive by including all possible decay chains of the stop. Thus we have included decays into  $t\tilde{\chi}_i^0$ ,  $b\tilde{\chi}_i^\pm$ ,  $t\tilde{g}$  and  $d\tilde{s}$ , of whom the first three are R-conserving decays while the last one is R-violating. The charginos, neutralinos or the gluino produced out of stop-decay have their usual cascades until the LSP (here  $\chi_1^0$ , the lightest neutralino) is reached. The  $\chi_1^0$  thereafter undergoes three-body RPV decays driven by  $\lambda''_{312}$ , to give rise to final states consisting leptons and jets of various multiplicities.

We observe that for the same values of  $(m_0, m_{1/2})$ , the mass and branching fractions of the stop may vary drastically with different values of  $(\tan \beta, A_0)$ . We shall choose  $\mu > 0$  for all the benchmark points as it is favoured by the constraint from the muon anomalous magnetic moment[23].

Since we explicitly want to study the situation in which the neutralino decays within the detector, the only available decay mode is  $\tilde{\chi}_1^0 \rightarrow t\bar{d}s(\bar{t}d\bar{s})$ . We therefore require that the neutralino mass be greater than the top mass to allow for a three-body decay. We fix  $m_{1/2} = 450$  GeV which gives  $M_{\tilde{\chi}_1^0} \sim 180$  GeV. We also choose the high scale value of

$\lambda''_{312} \sim 0.065$  such that it gives a value of 0.2 at the electroweak scale.

Figure 2 shows the branching fractions into various final states for three different choices of  $(\tan \beta, A_0)$ , namely,  $(5, -1500)$ ,  $(40, -1500)$  and  $(10, 0)$  for different stop masses, obtained by varying  $m_0$ . We notice that, for low  $m_0$ , the dominant decay mode is  $b\chi_2^+$  in the third case of Figure 2, while it is  $t\chi_1^0$  in the first two cases. We also notice that the decays into higher neutralinos and charginos open up earlier for  $\tan \beta = 40$  and compared to  $\tan \beta = 5$ .

The Tevatron reach for single stop production is about 450 GeV. We therefore start with a benchmark point with stop mass of 500 GeV, just beyond this reach (Point A). The major decay channels in this case are  $t\tilde{\chi}_1^0, b\tilde{\chi}_1^+$ . A stop mass of a TeV at the electroweak scale may be obtained by various configurations in the high-scale parameter space. However, from the above plots, one expects its decays to change significantly with different parameters. Our objective is to determine whether signal of resonant production of a stop of mass near a TeV can be probed irrespective of what the high-scale parameters are. For this, we fix  $M_{\tilde{t}_1} \sim 1$  TeV. We first look at the case with  $A_0 = -1500$ . We construct two benchmark points with  $\tan \beta = 5$  (Point B) and 40 (Point C) which correspond to the opposite ends of the allowed range in  $\tan \beta$ . We see that for a stop mass of 1 TeV, the decays into the higgsino-like  $\tilde{\chi}_2^+$  and  $\tilde{\chi}_3^0$  become dominant goes to high  $\tan \beta$ .

Similarly, we also look at a point with  $A_0 = 0$   $\tan \beta = 10$  (Point D). In this case, we find that the Higgsino channels open up fairly early and the dominant decay is  $b\tilde{\chi}_2^+$  followed by  $t\tilde{\chi}_3^0$ . As we shall see in the next section, this plays a crucial role in enhancing multi-lepton signals of a resonantly produced stop. Finally, since the decay into a top and a gluino does not open up until much higher stop masses, we also construct one point in which the stop decays dominantly into  $t\tilde{g}$  (Point E).

Points A, B and E correspond to the same value of  $(\tan \beta, A_0) = (5, -1500)$  and therefore provide a description of how the signal changes when only  $m_0$  is varied. This choice of parameters also corresponds to the most conservative case in terms of signal since the decay modes into the higher gauginos does not open for a large region in the parameter space. We will therefore use these points to obtain limits on  $\lambda''_{eff}$ .

We have tabulated the parameters and significant decay modes in Table 1. The benchmark points were generated with RPV renormalisation group running of couplings and masses using SOFTSUSY 3.0.2[24] and the RPV decays were calculated with the ISAWIG interface to Isajet[25].

The decay width of the stop in the R-parity violating channel  $ds$  depends only on  $\lambda''_{eff}$  and the stop mass. Therefore, the branching ratio into this channel for same values of  $\lambda''_{eff}$  and stop mass depends only on the decay widths of the other channels open at the same time. For the benchmarks under consideration,  $\tilde{\chi}_{1,2}^0$  and  $\tilde{\chi}_1^\pm$  have large gaugino fractions whereas  $\tilde{\chi}_{3,4}^0$  and  $\tilde{\chi}_2^\pm$  have large higgsino fractions. The large top mass means that stop coupling to higgsino-like chargino and neutralinos is large. Thus as soon as these decays become kinematically allowed, they quickly dominate over the decays into gaugino-like chargino and neutralinos. This can be seen for points B, C and D which have nearly identical stop masses and  $\sin^2 \theta_{\tilde{t}} (\lambda''_{312} = 0.2$  at electroweak scale for all points). Large  $\tan \beta$  opens up the  $b\tilde{\chi}_2^+$  mode early in point C as compared to point B and makes the



Point	$(m_0, \tan \beta, A_0)$	$M_{\tilde{t}_1}$	$\sin^2 \theta_{\tilde{t}}$	Dominant decay modes
A	(600,5,-1500)	508	0.88	$t\tilde{\chi}_1^0$ (0.35); $b\tilde{\chi}_1^+$ (0.19); $\bar{d}\bar{s}$ (0.48)
B	(1650,5,-1500)	1002	0.97	$t\tilde{\chi}_1^0$ (0.48); $t\tilde{\chi}_2^0$ (0.04); $b\tilde{\chi}_1^+$ (0.10); $\bar{d}\bar{s}$ (0.38)
C	(1570,40,-1500)	1002	0.95	$t\tilde{\chi}_1^0$ (0.35); $t\tilde{\chi}_2^0$ (0.05); $b\tilde{\chi}_1^+$ (0.12); $b\tilde{\chi}_2^+$ (0.21); $\bar{d}\bar{s}$ (0.27)
D	(1250,10,0)	1008	0.97	$t\tilde{\chi}_1^0$ (0.13); $t\tilde{\chi}_2^0$ (0.04); $t\tilde{\chi}_3^0$ (0.20); $t\tilde{\chi}_4^0$ (0.13); $b\tilde{\chi}_1^+$ (0.08); $b\tilde{\chi}_2^+$ (0.33); $\bar{d}\bar{s}$ (0.10)
E	(2450,5,-1500)	1404	0.99	$t\tilde{g}$ (0.39); $t\tilde{\chi}_1^0$ (0.15); $t\tilde{\chi}_2^0$ (0.02); $t\tilde{\chi}_3^0$ (0.08); $t\tilde{\chi}_4^0$ (0.07); $b\tilde{\chi}_1^+$ (0.02); $b\tilde{\chi}_2^+$ (0.17); $\bar{d}\bar{s}$ (0.11)

**Table 1:** Benchmark points and the dominant decay modes of the lighter stop.  $\lambda''_{312} = 0.2$ ,  $\mu > 0$  and  $m_{1/2} = 450$  GeV for all benchmark points.

branching fraction into  $ds$  for point C much lower. For point D, the branching fraction into higgsino-like chargino and neutralinos is larger than 60% and the RPV decay fraction is only about 10%. The  $\tilde{t} - t - \tilde{g}$  coupling comes from strong interactions and therefore the  $t\tilde{g}$  channel dominates whenever it becomes kinematically allowed (as in point E).

### 3. Event generation and selection

#### 3.1 Event generation

Signal events have been generated using HERWIG 6.510[26], and jets have been formed using anti- $k_T$  algorithm[27] from FastJet 2.4.1. SM backgrounds have been calculated using Alpgen 2.13[28] showered through Pythia [29] with MLM matching. We have used CTEQ6L1 parton distribution functions[30]. The renormalisation and factorisation scales have been set at the lighter stop mass ( $M_{\tilde{t}_1}$ ) for signal, while the default option in ALPGEN has been used for the backgrounds.

In R-parity conserving MSSM, the production of two heavy superparticles requires a large centre-of-mass energy at the parton level. This allows us to further suppress the SM background by applying cuts on global variables like the “effective mass” ( $M_{eff}$ ). Since we no longer have a large missing- $E_T$  and the energy scale of the resonant production process is not very high, the SM background cannot be suppressed so easily. We therefore concentrate on leptonic signals with or without b-tags to identify the signal over the background.

#### 3.2 Event selection

Decay of the lighter stop in this scenario can lead to a variety of final states. Out of them, we have chosen the following ones:

- Same-sign dileptons:  $SSD$
- Same-sign dileptons with one b-tagged jet:  $SSD + b$
- Trileptons:  $3l$

We do not consider the RPV dijet channel as a viable signature due to the enormous background from QCD processes. Similarly, we also omit opposite-sign dileptons due to large backgrounds from Drell-Yan,  $W^+W^-$ ,  $t\bar{t}$  etc.

We have imposed the following identification requirements on leptons and jets:

- **Leptons:** A lepton ( $l$ ) is considered isolated if (a) It is well separated from each jet ( $j$ ):  $\Delta R_{lj} > 0.4$ , (b) The total hadronic deposit within  $\Delta R < 0.35$  is less than 10 GeV. We consider only those leptons which fall within  $|\eta| < 2.5$  with  $p_T > 10$  GeV. Here,  $\Delta R = \sqrt{\Delta\eta^2 + \Delta\phi^2}$  where  $\eta$  is the pseudo-rapidity and  $\phi$  is the azimuthal angle.
- **Jets:** Jets have been formed using the anti- $k_T$  algorithm with parameter  $R = 0.7$ . We only retain jets with  $p_T > 20$  GeV and  $|\eta| < 2.5$ .
- **B-tagged jets:** A jet is b-tagged with probability of 0.5 if a b-hadron with  $50 < p_T < 100$  GeV lies within a cone of 0.7 from the jet axis. We have set the identification efficiency to be zero outside this window, in order to make our estimates conservative.

We also apply the following extra cuts on various final states to enhance the signal over background:

- **Cut 1: Lepton- $p_T$ :** We demand that the  $p_T$  of the leptons be greater than (40, 30) GeV for dilepton and (30, 30, 20) for trilepton channels. This cut removes the background from semileptonic decays of b quarks. It strongly suppresses the  $b\bar{b} + jets$ ,  $Wb\bar{b} + jets$  and  $t\bar{t} + jets$  background in the  $SSD$ -channel coming from semileptonic b-decays.
- **Cut 2: Missing  $E_T$ :** At least one lepton in the signal always comes from the decay of a W boson and is accompanied by a neutrino. We demand a missing- $E_T$  greater than 30 GeV from all events. This helps in reducing the probability of jets faking leptons. Missing- $E_T$  has been defined as  $|\vec{p}_{T,visible}|$ .
- **Cut 3: Jet  $p_T$ :** We demand that the number of jets,  $n_j \geq 2$  with  $p_T(j_1) > 100$  GeV and  $p_T(j_2) > 50.0$  GeV for  $SSD$  and  $SSD + b$ . This cut is useful when high stop mass is very high and the production cross section is very low.
- **Cut 4: Dilepton invariant mass:** We also apply a cut on dilepton invariant mass ( $M_{l_1, l_2}$ ) around Z-mass window ( $|M_{l_1, l_2} - M_Z| < 15.0$  GeV) for opposite sign dileptons of same flavour in trilepton events. This serves to suppress contribution from  $Zb\bar{b} + jets$  and  $WZ + jets$  background to trileptons.

Due to the Majorana nature of neutralinos,  $\lambda''$ -type interactions result in equal rates for  $tds$  and  $\bar{t}\bar{d}\bar{s}$ -type final states. Therefore, the most promising signals are those involving same-sign dileptons (SSD). This not only applies to  $\tilde{\chi}_1^0$  but also to the higher neutralinos produced in stop decay, whose cascades can give rise to W's. SSD have previously been used extensively for studying signals of supersymmetry [31, 32]. The most copious backgrounds to SSD processes come from the processes  $t\bar{t}$  and  $Wb\bar{b}$  due to one lepton from  $W$  and another

from semileptonic decays of the b-quark. There is also a potentially large contribution from  $b\bar{b}$  due to  $B^0 - \bar{B}^0$  oscillations along with semileptonic decays of both B-mesons. The effect of oscillations is simulated in the Pythia program. The  $p_T$ -cuts on leptons have been selected to minimise the background from heavy flavour decays [33]. We find that after the isolation and  $p_T$  cuts on leptons,  $Wb\bar{b}$  and  $b\bar{b}$  cross sections fall to sub-femtobarn levels.

We simulate the  $t\bar{t} + jets$  background up to two jets. The trilepton channel has another source of backgrounds in  $WZ + jets$ ; however, we have checked and found them to be negligibly small after applying all the cuts. We also generate  $Wt\bar{t} + jets$  and  $Zt\bar{t} + jets$  up to one jet.

It should be mentioned here that the dilepton and trilepton final states can also arise in the same scenario from the pair-production of superparticles. These include, for example, pair production of gluinos and electroweak production of chargino-neutralino pairs. Such contributions have been explicitly shown in the plots in section 4.

We also expect that the  $p_T$  distribution of the  $\tilde{t}_1$  becomes significantly harder if the NLO corrections are taken into account[12]. Our cuts on leptons have been designed to cut off the background from semileptonic b-decays by requiring the  $p_T$  to be about half the mass of the  $W$ . Therefore, if only the lepton cuts are used, we do not expect a large change in the efficiency of the cuts quoted in the next section.

## 4. Results

We present results using  $\lambda''_{312} = 0.2$ ; the predictions for other values of this coupling can be obtained through scaling arguments. If  $\lambda''_{312}$  is scaled by a factor of  $n$  then the production cross section as well as the decay width of the RPV channel scale by  $n^2$ . All other decay widths remain unchanged. If  $f$  is the branching fraction of  $\tilde{t} \rightarrow \bar{d}\bar{s}$  before scaling, then the signal rates in any other channel are scaled by a factor of

$$\frac{R_{new}}{R_{old}} = \frac{n^2}{(n^2 - 1)f + 1} \quad (4.1)$$

### 4.1 Limits at $\sqrt{s}=14, 10$ TeV

The numerical results for various signals corresponding to the five benchmark points for LHC running energy  $\sqrt{s} = 14, 10$  TeV are presented in Tables 2(for the  $SSD$  channel), 3 (for  $SSD + b$ ) and 4 (for  $3l$ ).

We can make the following observations from the numerical results:

- The final states  $SSD$  and  $SSD + b$  consistently have substantial event rates at both 14 and 10 TeV. Furthermore, the simultaneous observation of excesses in the  $SSD$  and  $SSD + b$  channel can serve as definite pointer to the production of a third generation squark.
- For point A, which is just above the Tevatron reach, we can achieve more than  $5\sigma$  significance in the  $SSD$  channel with just  $100 \text{ pb}^{-1}$  data at both 14 and 10 TeV. For point E, which has  $M_{\tilde{t}} = 1500 \text{ GeV}$ , we can reach  $3\sigma$  with  $1(3) \text{ fb}^{-1}$  and  $5\sigma$  with  $3(9)$

$SSD$ Point	14 TeV				10 TeV			
	Cut 0	Cut 1	Cut 2	Cut 3	Cut 0	Cut 1	Cut 2	Cut 3
A	884.8	496.8	<b>459.4</b>	41.0	540.1	312.7	<b>287.0</b>	15.1
B	64.7	43.7	<b>41.4</b>	19.3	30.6	21.0	<b>19.8</b>	9.6
C	83.0	51.5	<b>49.2</b>	25.8	40.1	25.6	<b>24.6</b>	12.5
D	145.4	71.9	<b>68.9</b>	41.1	65.1	32.3	<b>31.0</b>	19.0
E	29.8	16.5	15.9	<b>13.6</b>	10.7	5.8	5.6	<b>4.6</b>
$t\bar{t} + nj$	687.9	26.3	24.7	10.0	307.0	8.7	7.0	3.6
$Wt\bar{t} + nj$	17.0	9.2	8.7	5.2	7.6	3.9	3.7	2.0
$Zt\bar{t} + nj$	12.7	6.7	6.7	4.1	4.9	2.3	2.2	1.4
Total	717.6	42.2	40.1	19.3	319.5	14.9	12.9	7.0

**Table 2:** Effect of cuts on signal and SM background cross sections (in  $fb$ ) in the  $SSD$  channel at  $\sqrt{s} = 14, 10$  TeV. Cut 0 refers to all events passing the identification cuts. Cuts 1-3 are described in the text. The numbers corresponding to best significance ( $s/\sqrt{b}$ ) of the signal ( $s$ ) with respect to the background ( $b$ ) are highlighted in bold.

$SSD + b$ Point	14 TeV				10 TeV			
	Cut 0	Cut 1	Cut 2	Cut 3	Cut 0	Cut 1	Cut 2	Cut 3
A	243.2	134.7	<b>121.2</b>	14.1	158.7	67.5	<b>61.8</b>	6.6
B	13.8	9.6	<b>9.2</b>	4.7	8.3	6.0	<b>5.6</b>	2.8
C	25.3	15.2	<b>14.6</b>	8.0	12.7	7.8	<b>7.4</b>	4.1
D	47.9	23.9	<b>23.0</b>	15.2	21.2	9.9	<b>9.5</b>	6.3
E	11.3	6.2	6.0	<b>5.3</b>	4.1	2.2	2.1	<b>1.8</b>
$t\bar{t} + nj$	173.0	7.6	7.1	2.3	80.9	4.2	1.4	1.3
$Wt\bar{t} + nj$	6.7	0.8	0.8	0.6	4.0	2.1	1.9	1.3
$Zt\bar{t} + nj$	5.6	2.6	2.6	1.8	2.3	1.1	1.1	0.7
Total	185.3	11.0	10.5	4.7	87.2	7.4	4.4	3.3

**Table 3:** Same as Table 2, but for the  $SSD + b$  channel.

$fb^{-1}$  at 14(10) TeV. Therefore, we can conclude that the entire range from 500-1500 GeV can be successfully probed at the LHC for  $\lambda''_{312} = 0.2$ .

- Stops decaying into higher neutralinos and charginos make the total rates distinctly better. This is governed by Higgsino couplings and is therefore most prominent for high  $\tan\beta$  and low  $A_0$ . This effect is evident from the large event rates for point D. We can successfully probe this point in the  $SSD$  channel at  $5\sigma$  with less than  $1 fb^{-1}$  data at both 10 and 14 TeV runs.
- The trilepton final state occurs when the stop can decay into  $\chi_2^+$ ,  $\chi_{3,4}^0$  or  $\tilde{g}$ . Therefore, points A and B show almost no signal and Point D has the largest signal in this channel. This advantage is largely lost for benchmark point E due to the kinematic suppression in the stop production process.
- Reach for the LHC: Assuming the conservative case of ( $\tan\beta = 5$ ,  $A_0 = 0$ ), with

3l Point	14 TeV				10 TeV			
	Cut 0	Cut 1	Cut 2	Cut 4	Cut 0	Cut 1	Cut 2	Cut 4
A	49.1	2.8	2.8	0.0	18.0	1.1	1.1	0.0
B	2.0	0.6	0.6	0.1	1.1	0.2	0.2	0.0
C	13.7	9.1	9.1	1.1	6.5	3.7	3.7	0.6
D	48.2	29.6	29.0	8.6	24.1	14.5	14.1	4.5
E	9.3	5.7	5.5	3.0	3.4	2.1	2.1	1.2
$t\bar{t} + nj$	2.1	0.0	0.0	0.0	1.8	0.0	0.0	0.0
$Wt\bar{t} + nj$	4.1	2.5	2.4	1.0	2.2	1.4	1.4	0.6
$Zt\bar{t} + nj$	30.8	20.7	19.7	2.7	11.3	7.3	4.7	1.1
Total	37.0	23.2	22.1	3.7	15.3	8.7	6.1	1.7

**Table 4:** Effect of cuts on signal and SM background cross sections (in  $fb$ ) in the trilepton ( $3l$ ) channel at  $\sqrt{s} = 14, 10$  TeV. Cut 0 refers to all events passing the identification cuts. Cuts 1, 2 and 4 are described in the text. Cut 4 is necessary to eliminate background from  $WZ + jets$ .

10  $fb^{-1}$  luminosity, one can rule out  $\lambda''_{eff}$  greater than 0.007–0.045 (0.007–0.062) for stop masses between 500 and 1500 GeV at 95 % CL at  $\sqrt{s} = 14$  (10) TeV. A  $5\sigma$  discovery can be made in the same mass range for  $\lambda''_{eff}$  greater than 0.012–0.084 (0.012–0.12). However, we observe that the reach in stop mass does not decrease monotonously with stop mass. The opening of new decay channels can improve detection considerably. The statements about minimum value of  $\lambda''_{eff}$  that can be probed are therefore dependent on the particular decays of the stop. We therefore tabulate the minimum values of  $\lambda''_{eff}$  for each benchmark point at 10  $fb^{-1}$  for both 10 and 14 TeV in Table 5.

Point	14 TeV			10 TeV		
	95% CL	$3\sigma$	$5\sigma$	95 % CL	$3\sigma$	$5\sigma$
A	0.007	0.009	0.012	0.007	0.009	0.012
B	0.027	0.037	0.052	0.029	0.041	0.059
C	0.026	0.035	0.048	0.028	0.038	0.052
D	0.024	0.032	0.042	0.027	0.036	0.047
E	0.045	0.062	0.084	0.062	0.087	0.12

**Table 5:** Values of minimum  $\lambda''_{eff}$  that can be ruled out at 95% CL, probed at  $3\sigma$  or  $5\sigma$  with 10  $fb^{-1}$  of data at  $\sqrt{s} = 10, 14$  for each of the benchmark points. The significance used is  $s/\sqrt{b}$  where  $s$  is the signal and  $b$  is the background.  $s/b > 0.2$  in all cases.

In Figure 3, we present the effective mass distributions in  $SSD$  channel for all the benchmark points. Effective mass is defined as

$$M_{eff} = \sum_{jets} |\vec{p}_T| + \sum_{leptons} |\vec{p}_T| + \cancel{E}_T \quad (4.2)$$

The contributions from resonant stop production is superposed in the figures on the

SM backgrounds and also RPC superparticle production processes. The RPC contributions are much smaller and therefore do not provide a serious background to our signals.

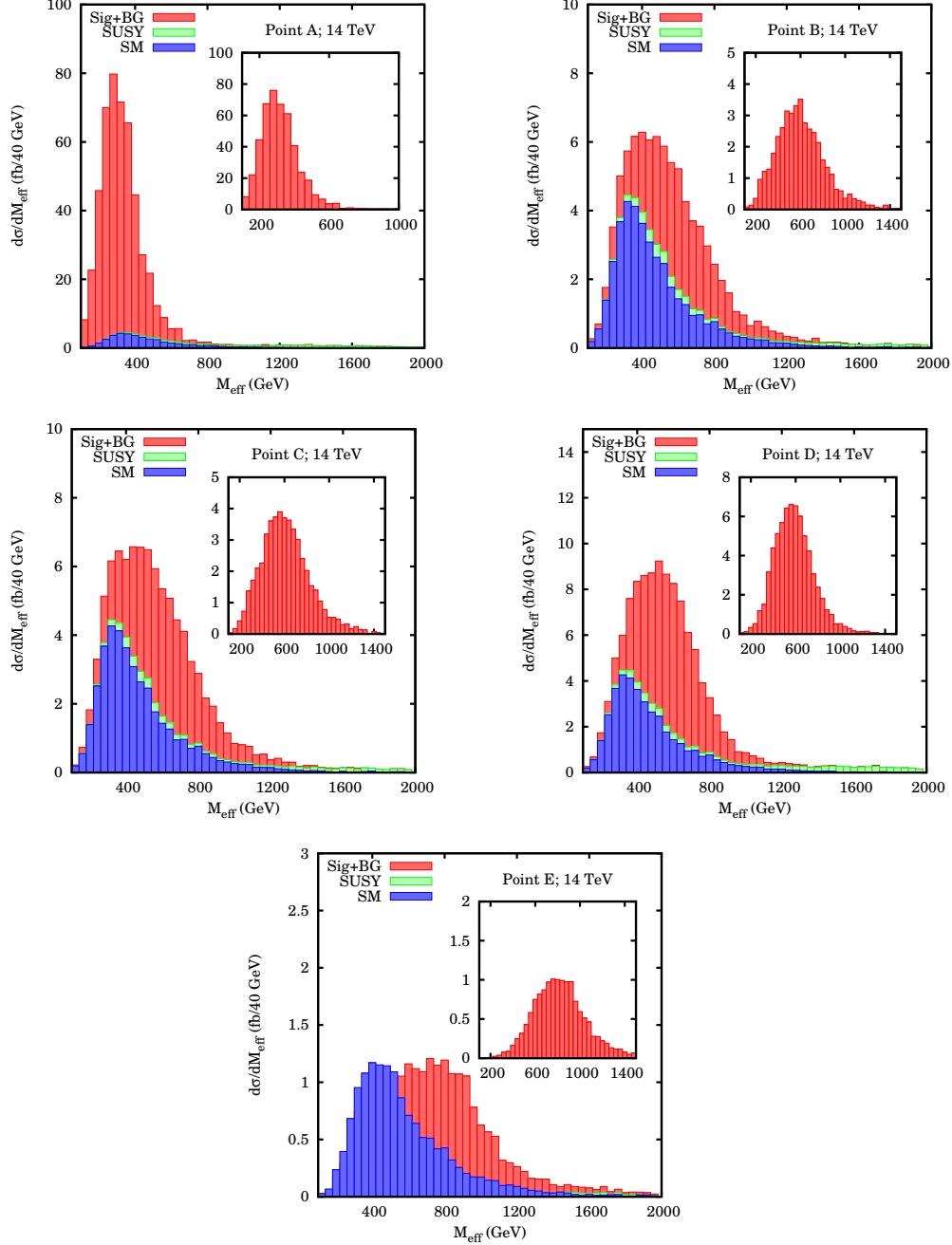


**Figure 3:**  $M_{\text{eff}}$  distributions at  $\sqrt{s} = 14$  TeV. “SM” is the contribution to the background from Standard Model processes. “SUSY” refers to the contribution from R-conserving production processes. The inset in each figure contains the distribution for the signal alone.

## 4.2 Observability at the early run of 7 TeV

The initial LHC run at  $\sqrt{s} = 7$  TeV will collect up to  $1 \text{ fb}^{-1}$  data. It will be difficult to observe RPV production of a 1 TeV stop at this energy. However, we can make useful comments for lower stop masses by looking at the  $SSD$  channel. We therefore look two benchmark points with low stop masses: the first is the ‘Point A’ described earlier and the second is similar to ‘Point D’ (with  $\tan \beta = 10$  and  $A_0 = 0$ ). Since the  $t\bar{t}$  backgrounds are much smaller at 7 TeV, we relax the jet- $p_T$  cuts. The high scale parameters, stop mass at electroweak scale and cut-flow table for signal as well as background are given in Table 6.

We conclude that we can rule out up to  $\lambda''_{eff} = 0.025$  for a stop mass of 500 GeV at 7 TeV with  $1 \text{ fb}^{-1}$  data and a  $5\sigma$  discovery can be made at stop mass 500 GeV for  $\lambda''_{eff} \geq 0.043$ . For the case  $\tan \beta = 10$  and  $A_0 = 0$ , the lowest possible theoretically allowed stop mass (with  $m_{1/2} = 450$  GeV) is 775 GeV and we can rule out up to  $\lambda''_{eff} = 0.054$  with  $1 \text{ fb}^{-1}$  data.

Point	$(\tan \beta, A_0, m_0)$	$M_{\tilde{t}_1}$	Cut 0	Cut 1	Cut 2
A	(5, -1500, 600)	508	283.3	158.6	147.5
D'	(10, 0, 100)	775	70.0	33.9	32.0
$t\bar{t} + nj$			116.0	3.7	3.5
$Wt\bar{t} + nj$			4.3	2.3	2.1
$Zt\bar{t} + nj$			1.8	0.9	0.8
Total			122.1	6.9	6.4

**Table 6:** The benchmark points for studying RPV stop production and the effect of cuts on signal and SM background cross sections (in  $fb$ ) in the  $SSD$  channel at  $\sqrt{s} = 7$  TeV. Cut 0 refers to all events passing the identification cuts. All other cuts are described in the text, we do not apply Cut 3.

## 4.3 Differentiating from R-conserving signals

We now address the question whether the signals we suggest can be faked by an R-parity conserving scenario in some other region(s) of the parameter space. One possible way that our signal may be mimicked is if a point in the mSUGRA parameter space (without RPV) gives similar kinematic distributions to any our benchmark points. More specifically, one may have a peak in the same region for the variable  $M_{eff}$ , defined in equation 4.2.

For each of our benchmark points A-D, an  $M_{eff}$  peak in the same region requires the strongly interacting particles to have masses in the range already ruled out by the Tevatron data[34]. In particular, they require the gluino mass  $M_{\tilde{g}} < 390$  GeV. Thus the question of faking arises only for benchmark point E, which represents the highest mass where the signals rates are appreciable.

We generate such a point (Point RC) with the parameters  $m_0 = 300$ ,  $m_{1/2} = 180$ ,  $A_0 = 0$ ,  $\tan \beta = 10$ ,  $\mu > 0$  and the resultant sparticle masses for coloured particles are  $M_{\tilde{g}} = 465$ ,  $M_{\tilde{q}} \sim 500$  GeV. The  $M_{eff}$  distributions for point E and point RC is shown in Figure 4. We present the following results at 14 TeV as an illustration. Distributions at 10 TeV are almost identical.

The missing  $E_T$  distribution is also not a good discriminator under such circumstances, as can be seen from Figure 4. This is because the neutrinos that contribute to missing- $E_T$  in the RPV case are highly boosted due to the large masses of the particles produced in the initial hard scattering. Thus, the  $E_T$  spectrum is actually harder for the RPV case even though the RPC case has a stable massive LSP. However, as the resultant spectrum is quite light, the RPC production cross section ( $\sim 40$  pb) is about two orders of magnitude greater than the RPV case with  $\lambda''_{312} = 0.2$  ( $\sim 480$  fb). Consequently, the rate of the SSD signals, for example, are much higher in the R-conserving scenario ( $\sim 34$  fb) as compared to those from point E ( $\sim 14$  fb). For values of  $\lambda''_{312} < 0.2$ , we can therefore make a reliable distinction simply based on the number of events expected in the SSD channel.

Another possible discriminator is the charge asymmetry. In the  $SSD$  channel, one can look at the ratio of negative to positive  $SSD$   $\frac{N^{--}}{N^{++}}$ . The fraction of  $ds \rightarrow \tilde{t}_1^*$  is more than the charge conjugate process  $\bar{d}\bar{s} \rightarrow \tilde{t}_1$  due to the difference in parton distributions of  $d$  and  $\bar{d}$  in the proton. Therefore, one expects extra negative sign leptons than positive ones. Whereas in the RPC case, since most of the  $SSD$  contribution comes from  $\tilde{g}\tilde{g}$  production, we do not expect a large asymmetry. In our illustration, we see that this ratio is 2.7 (1.4) for the RPV (RPC) case.

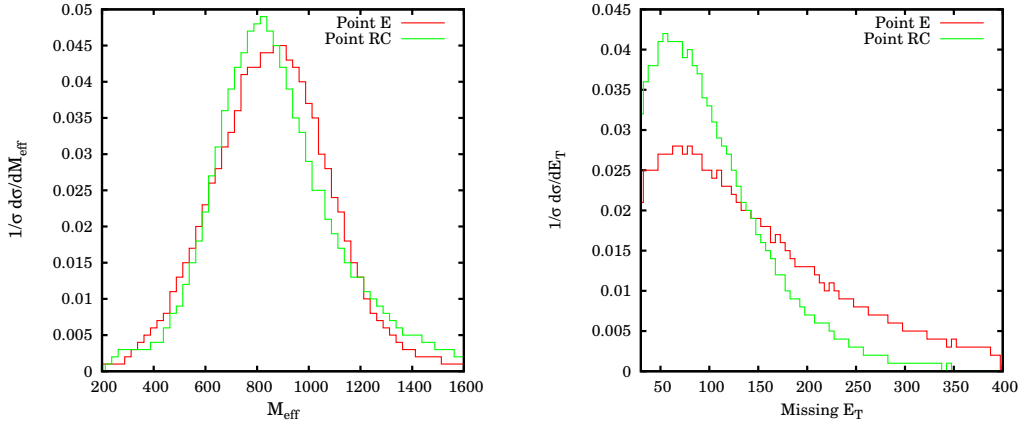


**Figure 4:** The normalised effective mass ( $M_{eff}$ ) and missing energy ( $E_T$ ) distributions in the  $SSD$  channel for Point E and an Point RC. Point RC has been generated using  $m_0 = 300, m_{1/2} = 180; A_0 = 0, \tan\beta = 10$  and  $\mu > 0$ . The gluino mass is 465 GeV.

## 5. Non- $\tilde{\chi}_1^0$ LSPs

For RPV models, the restriction of having an uncharged LSP no longer exists. A significant region of the mSUGRA parameter space with low  $m_0$  corresponds to a stau ( $\tilde{\tau}$ ) LSP. With only  $\lambda''_{312}$ -type couplings present, the stau can only decay via off-shell  $\tilde{\chi}_1^0$  and  $\tilde{t}$  propagators into the four body decay ( $\tilde{\tau} \rightarrow \tau t d s$ ) if its mass,  $m_{\tilde{\tau}} > m_{top}$  or via the five body decay ( $\tilde{\tau} \rightarrow \tau b W d s$ ) if  $m_{\tilde{\tau}} < m_{top}$  where the top propagator is also off-shell. The four-body decays of the stau in lepton-number violating scenarios was calculated in [35]. Since the intermediate  $\tilde{\chi}_1^0$  is of Majorana character, we can always have one lepton of either sign



from LSP decay via the  $W$  from an on-shell or off-shell top. Thus, for various types of  $\tilde{t}$  decays, the following situations may arise:

- For decays of  $t\tilde{\chi}_i^0$ -type, we can still have same-sign dileptons with one lepton from top decay and the other from the decay of the LSP.
- For decays of type  $b\tilde{\chi}_i^\pm$  with  $\chi_i^\pm \rightarrow W^\pm \tilde{\chi}_1^0 + X$ , we have  $\tilde{\chi}_1^0 \rightarrow \tau\tilde{\tau}$  and the SSD come from  $W^\pm$  and LSP decay respectively.
- For decays of the type  $\tilde{t} \rightarrow b\tilde{\chi}_i^+$  with  $\tilde{\chi}_i^+ \rightarrow \nu_\tau \tilde{\tau} + X$ , we may still get SSD from leptonic decay of the  $\tau$  in the  $\tilde{\tau}$  decay. If  $\tau$ -identification is used, final states of the type same-sign ( $\tau + e/\mu$ ) may be considered.
- Since the stau has to decay via four- or five-body processes, it is possible that the lifetime of the  $\tilde{\tau}$  is large and it is stable over the length scale of the detector. In this case, it will leave a charged track like a muon and one can look at same-sign leptons with this “muon” as one of the leptons. It is also possible that the lifetime is large but the stau still decays within the detector. In this case, a displaced vertex can be observed in the detector.

We leave the detailed simulation of all scenarios of resonant stop production with stau LSP to a future study.

Another possibility that arises with a large  $\lambda_{312}''$  is of having a stop LSP. In this case however, the decay will be almost entirely via the RPV  $\bar{d}\bar{s}$  di-jet channel. The overwhelmingly large dijet backgrounds at the LHC would most likely make this situation unobservable.

## 6. Summary and Conclusion

We have performed a detailed analysis of resonant stop production at the LHC, both for the 10 and 14 TeV runs, for values of the baryon number violating coupling  $\lambda_{312}''$  an order of magnitude below the current experimental limit. Benchmark points have been chosen for this purpose, which start just beyond the reach of the Tevatron and end close at the LHC search limit. We find that the same-sign dilepton final states, both with and without a tagged b, are most helpful in identifying the signal. The trilepton signals can also be sometimes useful, especially when decays of the resonant into higher neutralinos, the heavier chargino or the gluino open up. At 14(10) TeV, we can probe stop masses up to 1500 GeV and values of  $\lambda_{eff}''$  down to 0.05(0.06) depending on the combination of various SUSY parameters. For cases of stop mass below a TeV, the effective mass distributions can enable us to distinguish between the resonant process and contributions from R-parity conserving SUSY processes. For higher stop masses, one has to rely on cross sections or the charge asymmetry.

We have used a particular B-violating coupling, namely,  $\lambda_{312}''$ . One can also have resonant stop production driven by  $\lambda_{313}''$  and  $\lambda_{323}''$ . In either of these cases, one expects

a larger abundance of  $b$  quarks in the final state. However, there is a suppression in the production rates due to the  $b$ -distribution function in the proton.

In conclusion, resonant stop production is a potentially interesting channel to look for SUSY in its baryon-number violating incarnation. Values of the  $B$ -violating coupling(s) more than an order below the current experimental limits can be definitely probed at the LHC, both at 10 and 14 TeV. If such interactions really exist, our suggested strategy can not only yield detectable event rates but also point towards resonant production as opposed to pair-production of SUSY particles.

## Acknowledgements

We would like to thank Satyaki Bhattacharya, Gobinda Majumdar, Bruce Mellado and Satyanarayan Mukhopadhyay for helpful discussions and comments. ND thanks the Indian Association for the Cultivation of Science for hospitality while part of this work was carried out. This work was partially supported by funding available from the Department of Atomic Energy, Government of India for the Regional Centre for Accelerator-based Particle Physics, Harish-Chandra Research Institute. Computational work for this study was partially carried out at the cluster computing facility of Harish-Chandra Research Institute (<http://cluster.mri.ernet.in>).

## References

- [1] H. P. Nilles, *Supersymmetry, Supergravity and Particle Physics*, *Phys. Rept.* **110** (1984) 1–162.
- [2] G. L. Kane, (ed. ), *Perspectives on supersymmetry*. World Scientific, Singapore, 1998.
- [3] R. Barbier *et al.*, *R-parity violating supersymmetry*, *Phys. Rept.* **420** (2005) 1–202, [[hep-ph/0406039](#)].
- [4] F. Zwirner, *Observable Delta B=2 Transitions Without Nucleon Decay in a Minimal Supersymmetric Extension of the Standard Model*, *Phys. Lett.* **B132** (1983) 103–106.
- [5] H. K. Dreiner and G. G. Ross, *R-parity violation at hadron colliders*, *Nucl. Phys.* **B365** (1991) 597–613.
- [6] R. Barbieri and A. Masiero, *Supersymmetric Models with Low-Energy Baryon Number Violation*, *Nucl. Phys.* **B267** (1986) 679.
- [7] G. Bhattacharyya, D. Choudhury, and K. Sridhar, *New LEP bounds on B violating scalar couplings: R-parity violating supersymmetry or diquarks*, *Phys. Lett.* **B355** (1995) 193–198, [[hep-ph/9504314](#)].
- [8] K. Agashe and M. Graesser, *R-parity violation in flavor changing neutral current processes and top quark decays*, *Phys. Rev.* **D54** (1996) 4445–4452, [[hep-ph/9510439](#)].
- [9] B. C. Allanach, A. Dedes, and H. K. Dreiner, *Bounds on R-parity violating couplings at the weak scale and at the GUT scale*, *Phys. Rev.* **D60** (1999) 075014, [[hep-ph/9906209](#)].
- [10] E. L. Berger, B. W. Harris, and Z. Sullivan, *Single-top-squark production via R-parity-violating supersymmetric couplings in hadron collisions*, *Phys. Rev. Lett.* **83** (1999) 4472–4475, [[hep-ph/9903549](#)].

- [11] E. L. Berger, B. W. Harris, and Z. Sullivan, *Direct probes of R-parity violating supersymmetric couplings via single top squark production*, *Phys. Rev.* **D63** (2001) 115001, [[hep-ph/0012184](#)].
- [12] T. Plehn, *Single stop production at hadron colliders*, *Phys. Lett.* **B488** (2000) 359–366, [[hep-ph/0006182](#)].
- [13] H. Baer, C. Kao, and X. Tata, *Impact of R-parity violation on supersymmetry searches at the tevatron*, *Phys. Rev.* **D51** (1995) 2180–2186, [[hep-ph/9410283](#)].
- [14] B. C. Allanach *et al.*, *Measuring supersymmetric particle masses at the LHC in scenarios with baryon-number R-parity violating couplings*, *JHEP* **03** (2001) 048, [[hep-ph/0102173](#)].
- [15] B. C. Allanach, A. J. Barr, M. A. Parker, P. Richardson, and B. R. Webber, *Extracting the flavour structure of a baryon-number R-parity violating coupling at the LHC*, *JHEP* **09** (2001) 021, [[hep-ph/0106304](#)].
- [16] H. K. Dreiner and S. Grab, *All Possible Lightest Supersymmetric Particles in R-Parity Violating mSUGRA*, *Phys. Lett.* **B679** (2009) 45–50, [[arXiv:0811.0200](#)].
- [17] J. M. Butterworth, J. R. Ellis, A. R. Raklev, and G. P. Salam, *Discovering baryon-number violating neutralino decays at the LHC*, *Phys. Rev. Lett.* **103** (2009) 241803, [[arXiv:0906.0728](#)].
- [18] T. Plehn, M. Spannowsky, M. Takeuchi, and D. Zerwas, *Stop Reconstruction with Tagged Tops*, [[arXiv:1006.2833](#)].
- [19] G. L. Kane, C. F. Kolda, L. Roszkowski and J. D. Wells, *Study of constrained minimal supersymmetry*, *Phys. Rev.* **D49** (1994) 6173–6210. [[hep-ph/9310291](#)].
- [20] **R parity Working Group** Collaboration, B. Allanach *et al.*, *Searching for R parity violation at Run II of the Tevatron*, [hep-ph/9906224](#).
- [21] **The ATLAS** Collaboration, G. Aad *et al.*, *Expected Performance of the ATLAS Experiment - Detector, Trigger and Physics*, [arXiv:0901.0512](#).
- [22] P. Nath, R. L. Arnowitt, and A. H. Chamseddine, *Applied N=1 Supergravity*. World Scientific, Singapore, 1984.
- [23] U. Chattopadhyay and P. Nath, *Upper limits on sparticle masses from g-2 and the possibility for discovery of SUSY at colliders and in dark matter searches*, *Phys. Rev. Lett.* **86** (2001) 5854–5857, [[hep-ph/0102157](#)].
- [24] B. C. Allanach and M. A. Bernhardt, *Including R-parity violation in the numerical computation of the spectrum of the minimal supersymmetric standard model: SOFTSUSY3.0*, *Comput. Phys. Commun.* **181** (2010) 232–245, [[arXiv:0903.1805](#)].
- [25] F. E. Paige, S. D. Protopopescu, H. Baer, and X. Tata, *ISAJET 7.69: A Monte Carlo event generator for p p, anti-p p, and e+ e- reactions*, [hep-ph/0312045](#).
- [26] G. Corcella *et al.*, *HERWIG 6.5 release note*, [hep-ph/0210213](#).
- [27] M. Cacciari, G. P. Salam, and G. Soyez, *The anti- $k_t$  jet clustering algorithm*, *JHEP* **04** (2008) 063, [[arXiv:0802.1189](#)].
- [28] M. L. Mangano, M. Moretti, F. Piccinini, R. Pittau, and A. D. Polosa, *ALPGEN, a generator for hard multiparton processes in hadronic collisions*, *JHEP* **07** (2003) 001, [[hep-ph/0206293](#)].

- [29] T. Sjostrand, S. Mrenna, and P. Z. Skands, *PYTHIA 6.4 Physics and Manual*, *JHEP* **05** (2006) 026, [[hep-ph/0603175](#)].
- [30] J. Pumplin *et al.*, *New generation of parton distributions with uncertainties from global QCD analysis*, *JHEP* **07** (2002) 012, [[hep-ph/0201195](#)].
- [31] R. M. Barnett, J. F. Gunion, and H. E. Haber, *Discovering supersymmetry with like sign dileptons*, *Phys. Lett.* **B315** (1993) 349–354, [[hep-ph/9306204](#)].
- [32] H. K. Dreiner, M. Guchait, D. P. Roy, *Like sign dilepton signature for gluino production at CERN LHC with or without R conservation*, *Phys. Rev.* **D49** (1994) 3270–3282. [[hep-ph/9310291](#)].
- [33] Z. Sullivan and E. L. Berger, *Isolated leptons from heavy flavor decays: Theory and data*, *Phys. Rev.* **D82** (2010) 014001, [[arXiv:1003.4997](#)].
- [34] **Particle Data Group** Collaboration, C. Amsler *et al.*, *Review of particle physics*, *Phys. Lett.* **B667** (2008) 1.
- [35] H. K. Dreiner, S. Grab, and M. K. Trenkel, *Stau LSP Phenomenology: Two versus Four-Body Decay Modes. Example: Resonant Single Slepton Production at the LHC*, *Phys. Rev.* **D79** (2009) 016002, [[arXiv:0808.3079](#)].